Single event leak detection in a pipeline using the first three resonant responses

Jinzhe Gong[1], Martin F. Lambert[2], Angus R. Simpson[3], Aaron C. Zecchin[4]

[1]PhD Candidate; School of Civil, Environmental and Mining Engineering, University of Adelaide, SA 5005, Australia; Email: jinzhe.gong@adelaide.edu.au

[2]Professor; School of Civil, Environmental and Mining Engineering, University of Adelaide, SA 5005, Australia; Email: martin.lambert@adelaide.edu.au

[3]Professor; School of Civil, Environmental and Mining Engineering, University of Adelaide, SA 5005, Australia; Email: angus.simpson@adelaide.edu.au

[4]Lecturer; School of Civil, Environmental and Mining Engineering, University of Adelaide, SA 5005, Australia; Email: aaron.zecchin@adelaide.edu.au

Abstract

Hydraulic transients (water hammer waves) can be used to excite a pressurized pipeline, yielding the frequency response diagram (FRD) of the system. The FRD of a pipeline system is useful for condition assessment and fault detection, because it is closely related to the physical properties of the pipeline. Most previous FRD-based leak detection techniques use the sinusoidal leak-induced pattern recorded on the FRD, either shown on the resonant responses or the anti-resonant responses. In contrast, the technique reported in the current paper only uses the responses at the first three resonant frequencies to determine the location and size of a leak. The bandwidth of the excitation only needs to be five times that of the fundamental frequency of the tested pipeline, which is much less than the requirement in conventional FRD-based techniques. Sensitivity analysis and numerical simulations are performed to assess the robustness and applicable range of the proposed leak location technique. The proposed leak location technique is verified by both numerical simulations and using an experimental FRD obtained from a laboratory pipeline.

Keywords: pipelines; fluid transients; water hammer; water distribution systems; leak detection; frequency response diagram; harmonic analysis

Introduction

With rapid population growth, urbanization and industrialization, providing adequate water for domestic and industry use is increasingly becoming a challenge for water authorities around the world. Resources of fresh water are limited or even scarce in some countries, however, for almost every city, only part of the treated water is delivered to consumers successfully, since a large amount of water is lost during transmission.

The amount of water lost during transmission varies between systems, from lower than 10 % in well maintained systems such as those in The Netherlands (Beuken et al. 2006) to more than 50 % in some undeveloped countries or regions (Mutikanga et al. 2009). According to publications released by the International Water Association (Lambert 2002) and the Asian Development Bank (McIntosh and Yniguez 1997), ‘non-revenue water’ (NRW) or ‘unaccounted for water’ (UFW) is between 20 % to 40 % for most countries or cities investigated. Among various reasons for the water loss, leakage is considered to be the major one (Nixon and Ghidaoui 2006; Colombo et al. 2009).

In addition to water loss, leakage also costs extra energy for water treatment, storage and pumping (Colombo and Karney 2002). Moreover, leaks may lead to water quality problems, because toxins and bacteria can be introduced into water distribution systems via leaks in low pressure conditions during hydraulic transients (Karim et al. 2003; Colombo et al. 2009; Meniconi et al. 2011; Collins et al. 2012). As a result, leak detection in water distribution systems is of great interest in both industry and academic areas (Puust et al. 2010).

In the past two decades, a number of leak detection techniques have been developed, including acoustic techniques (Fuchs and Riehle 1991; Tafuri 2000), ground penetrating radar (Eiswirth and Burn 2001), electromagnetic techniques (Goh et al. 2011), fiber optic sensing (Inaudi et al. 2008), and hydraulic transient-based techniques (Colombo et al. 2009; Puust et al. 2010). A major advantage of the transient-based methods is that the information of a long pipeline (usually thousands meters) can be obtained efficiently and cost-effectively, because transient waves travel at high speed along fluid-filled pipes. Up to now, intensive simplified numerical simulations, some elaborately controlled laboratory experiments and a few field tests have been conducted for leak detection using transient-based techniques (Colombo et al. 2009; Puust et al. 2010).

The existing transient-based leak detection techniques can be divided into two categories: the time-domain techniques and the frequency-domain techniques. In the time domain, leak-induced reflections are observed as discontinuities in the pressure traces measured along the pipe. A few leak detection techniques have been developed based on time-domain phenomena (Jönsson and Larson 1992; Brunone 1999), which are complicated by the fact that the size and shape of a leak-induced reflection not only depend on the properties of the leak, but also relate to the input signal (Lee et al. 2007). For example, using a positive step transient wave as the input, the leak-induced reflections are shown as a small negative step in the measured pressure trace; while when a pulse input is injected, the leak-induced reflections are also pulses. By using signal processing, a leak location can be determined irrespective of the characteristics of the input signal. For example, the use of the wavelet analysis (Ferrante and Brunone 2003a) or the impulse response function (IRF) of the pipeline can improve the estimation of the leak location (Vítkovský et al. 2003b; Lee et al. 2007). However, difficulties exist in real world applications, where leak-induced reflections are usually small in magnitude, and they can be hard to distinguish from the reflections introduced by other hydraulic components, such as joints, junctions, and entrapped air.

Several transient-based leak detection techniques have been developed in the frequency domain, based on analyzing the frequency response function (FRF) or the frequency response diagram (FRD) of a pipeline system. The FRF of a pipeline system is the Fourier transform of the IRF, which describes the magnitude of the system response to each oscillatory excitation at a specific frequency, and the FRD is the plot of a FRF. The FRF or FRD is dependent on the physical configuration of the pipeline system, such as the boundary condition, the length, the location and size of the leak. As a result, the FRF or FRD can be used for leak detection.

Jönsson and Larson (1992) first proposed that it is possible to distinguish the leak-induced reflections in the spectrum at a frequency corresponding to the leak location. Mpesha et al. (2001) proposed that the FRD of a pipeline with leaks had additional resonant pressure amplitude peaks, and a method using the FRD was presented for detecting and locating leaks. Ferrante and Brunone (2003b) demonstrated that Fourier transform of transient pressure does not show further peaks unless leak size is larger than a critical value.

Covas et al. (2005) proposed a *standing wave difference method*, which uses the spectral analysis of an FRD to determine the leak-resonance frequency and indicate the leak location. However, two locations are estimated for a single leak, with one of them an alias and undistinguishable.

Lee et al. (2005a) proposed a *resonance peak-sequencing method* for leak location. The resonant responses in a FRD (peaks at the odd harmonics of the pipeline fundamental frequency) are ranked in order of magnitude. The rank sequence is indicative to the dimensionless leak location range, and the size of the leak has no effect on the order of the peaks. For example, using the rank sequence of the first three resonant peaks, the leak can be located to one of the six unequal ranges along the pipe, but the exact location cannot be pinpointed.

In the same year, Lee et al. (2005b) proposed a technique for leak location and size estimation using the sinusoidal leak-induced pattern shown on the resonant responses (frequency responses at the odd harmonics). The period and phase of the sinusoidal leak-induced pattern is indicative of the leak location, while the amplitude is related to the leak size. One year later, laboratory experiments were conducted by the same authors, which verified the odd harmonics-based leak detection technique (Lee et al. 2006). The experimental FRD were affected by the frequency-dependent behavior resulting from unsteady friction. In order to produce an accurate estimation of the oscillation frequency and phase, a least squares regression algorithm was adapted to fit a cosine function to the inverted resonant responses. However, up to 10 coefficients need to be calibrated, which requires at least 10 resonant responses to yield a determined system for the regression process.

Sattar and Chaudhry (2008) suggested a similar leak detection method but using the leak-induced pattern on the anti-resonant responses (frequency responses at the even harmonics). The anti-resonant responses can be hard to measure accurately in practice, because they are usually low in amplitude.

The odd harmonics-based leak detection technique was extended to complex series pipe systems by Duan et al. (2011), in which the results of analytical analysis and numerical simulations suggest that internal junctions of series pipe sections can change the location of the resonant peaks, but have little impact on the period and phase of the leak-induced sinusoidal pattern.

Although the existing odd harmonics-based leak detection technique (Lee et al. 2005b; Duan et al. 2011) has its advantages, two major limitations are obstacles for real world applications. Firstly, a significant number of resonant responses need to be known, in order to provide sufficient information to identify the period and phase of the sinusoidal leak-induced pattern. This in turn requires the input signal to have a wide bandwidth that covers a significant number of harmonics of the pipeline's fundamental frequency. However, due to limitations in the maneuverability of existing transient generators, it is difficult to obtain a wide bandwidth input with enough signal-to-noise-ratio (SNR). Secondly, the distortion caused by the frequency-dependent behavior of real pipelines, such as the effects of unsteady friction, needs to be corrected in order to give a better estimation of the amplitude, period and phase of the sinusoidal leak-induced pattern. The frequency-dependent behavior of real pipelines is complicated, and more distortion is expected in the response at higher resonant frequencies.

The research presented in this paper proposes a novel FRD-based leak detection technique that is not affected significantly by problems with either the bandwidth of the input or distortion due to unsteady friction. Only the first three resonant responses recorded in a FRD (which are the responses at the first three odd harmonics), are used to estimate the location and size of a single leak. The bandwidth of the input signal only needs to be greater than the third resonant frequency of the pipeline, which is five times the fundamental frequency. In addition, the effects of unsteady friction are usually not significant on the first three resonances, and the new leak location algorithm is robust to measurement errors (as shown in the sensitivity analysis in a latter section), so that the procedure for correction can be avoided. This new technique is verified by both numerical simulations and laboratory experiments.

Frequency response equations for a single pipe with a leak

This section reviews the frequency response equations for a single pipeline with a leak, which are the basis of most frequency-domain transient-based leak detection techniques. The reservoir-pipeline-valve (RPV) configuration is adopted, where two possible boundary conditions are discussed and compared.

System configurations

Typically, to extract the FRD of a pipeline, systems with two types of configuration can be used: the reservoir-pipeline-valve (RPV) system and the reservoir-pipeline-reservoir (RPR) system (Lee et al. 2006). The fundamental frequency of a RPV system is half that of a RPR system (Lee et al. 2006). As a result, the RPV system requires a smaller bandwidth for the input signal to cover the same number of resonant frequencies, and this type of configuration is the focus of the current research. A typical RPV system for leak detection is given in Fig. 1, where H_r represents the head of the reservoir; L is the total length of the pipe; L_1 and L_2 are the length of the pipe sections upstream and downstream of the leak, respectively. A pressure transducer is located at the end of the pipe to achieve the highest signal-to-noise ratio (Lee et al. 2006).

Pipeline systems with a RPV configuration can have two possible boundary conditions: the *RPV-High Loss Valve* boundary condition and the *RPV-Closed Valve* boundary condition. For RPV-High Loss Valve systems, the in-line valve has a small opening to achieve a high value of hydraulic impedance. The downstream side of the in-line valve can be connected to the atmosphere or a constant head reservoir. For *RPV-Closed Valve* systems, the in-line valve is fully closed to form a dead end.

The frequency responses equations for pipelines with the *RPV-High Loss Valve* and the *RPV-Closed Valve* boundary conditions are given below in sequence. The *RPV-Closed Valve* boundary condition can be regarded as a special case of the *RPV-High Loss Valve* boundary condition, where the opening of the valve is extremely small. The limitations and benefits of the *RPV-Closed Valve* boundary condition are analyzed and presented.

Frequency response equations for RPV-High Loss Valve systems

The frequency response equation of a pipeline system can be derived from the transfer matrix method (Chaudhry 1987; Wylie and Streeter 1993). The transfer matrix for an intact pipe section is given as

$$\begin{Bmatrix} q \\ h \end{Bmatrix}^{n+1} = \begin{bmatrix} \cosh(\mu L_i) & \dfrac{-1}{Z_P}\sinh(\mu L_i) \\ -Z_P \sinh(\mu L_i) & \cosh(\mu L_i) \end{bmatrix} \begin{Bmatrix} q \\ h \end{Bmatrix}^{n} \tag{1}$$

where q and h are complex discharge and head at either end of the pipe section; the superscripts n and $n+1$ represent the upstream and downstream positions respectively; L_i is the length of this pipe section; $Z_P = \mu a^2 / (j\omega g A)$ is the characteristic impedance of the pipe; μ is the propagation operator given by $\mu = \sqrt{-\omega^2 / a^2 + jgA\omega R / a^2}$, in which ω is the angular frequency; a is the wave speed; $j = \sqrt{-1}$ is the imaginary unit; g is the gravitational acceleration; A is the cross-sectional area of the pipe; and R is a linearised resistance term. For turbulent flow and steady friction $R = R_s = fQ_0 / (gDA^2)$, where f is the Darcy-Weisbach friction factor; Q_0 is the steady-state flow rate; and D is the inside diameter of the pipeline. If unsteady friction is included, an additional component R_{us} needs to be added into the linearised resistance term, i.e. $R = R_s + R_{us}$. Unsteady friction is studied in detail in the *numerical verification* section presented latter in this paper.

To highlight the impact of a leak on the frequency response, the pipeline is assumed to be frictionless in the following derivation. The transfer matrix for a frictionless and intact pipe is given as

$$\begin{Bmatrix} q \\ h \end{Bmatrix}^{n+1} = \begin{bmatrix} \cos\left(\frac{L_i\omega}{a}\right) & -\frac{j}{Z_C}\sin\left(\frac{L_i\omega}{a}\right) \\ -jZ_C\sin\left(\frac{L_i\omega}{a}\right) & \cos\left(\frac{L_i\omega}{a}\right) \end{bmatrix} \begin{Bmatrix} q \\ h \end{Bmatrix}^{n} \tag{2}$$

where $Z_C = a/(gA)$ is the characteristic impedance of a frictionless pipeline.

The matrix for a leak is

$$\begin{Bmatrix} q \\ h \end{Bmatrix}^{n+1} = \begin{bmatrix} 1 & -\frac{1}{Z_L} \\ 0 & 1 \end{bmatrix} \begin{Bmatrix} q \\ h \end{Bmatrix}^{n} \tag{3}$$

where $Z_L = 2H_{L0}/Q_{L0}$ is the impedance of the leak in the steady state, in which H_{L0} and Q_{L0} are the steady-state head and discharge at the leak.

An in-line valve can be used to generate steady oscillatory flow, where the transfer matrix is given as

$$\begin{Bmatrix} q \\ h \end{Bmatrix}^{n+1} = \begin{bmatrix} 1 & 0 \\ -Z_V & 1 \end{bmatrix} \begin{Bmatrix} q \\ h \end{Bmatrix}^{n} + \begin{Bmatrix} 0 \\ \frac{2\Delta H_{V0}\Delta\tau}{\tau_0} \end{Bmatrix} \tag{4}$$

where $Z_V = 2\Delta H_{V0}/Q_{V0}$ is the impedance of the in-line valve at the steady state, in which ΔH_{V0} and Q_{V0} are the steady-state head loss across the valve and the flow through the valve, respectively; τ_0 is the dimensionless valve opening size at the steady state; and

$\Delta\tau$ is the amplitude of the dimensionless valve opening perturbation that generates the transients.

The matrices for all the components along a pipeline can be multiplied together from the downstream to upstream boundary to form an overall transfer matrix. At the upstream face of the in-line valve (where the transducer is located), the magnitude of the head response at resonant frequencies (odd harmonics) is given as

$$|h_{odd}| = \frac{2\Delta H_{V0}\Delta\tau/\tau_0}{1+\frac{Z_V}{2Z_L}\left[1-\cos\left(\pi x_L^* \omega_r^{odd}\right)\right]} \tag{5}$$

where x_L^* is the dimensionless leak location that is defined as $x_L^* = L_1/L$; and ω_r^{odd} represents the relative angular frequency for the odd harmonics, which is given as $\omega_r^{odd} = \omega^{odd}/\omega_{th}$ = 1, 3, 5…, where ω^{odd} represents the angular frequency for the odd harmonics; and $\omega_{th} = a\pi/(2L)$ is the fundamental angular frequency of the RPV system.

In practice, it is difficult to control the oscillatory perturbation of an in-line valve. Instead, a side-discharge valve located upstream of and adjacent to the in-line valve can be used to generate the transients (Lee et al. 2006). The side-discharge valve can be modeled as a point where a discharge perturbation takes place:

$$\begin{Bmatrix} q \\ h \end{Bmatrix}^{n+1} = \begin{bmatrix} 1 & 0 \\ 0 & 1 \end{bmatrix} \begin{Bmatrix} q \\ h \end{Bmatrix}^{n} + \begin{Bmatrix} \hat{q} \\ 0 \end{Bmatrix} \tag{6}$$

where $\hat{q}$ represents the discharge perturbation at the side-discharge valve.

Once a side-discharge valve is used to generate the transients, the in-line valve can have a constant opening, of which the transfer matrix can be obtained from Eq. (4) by removing the last column vector on the right hand side. Then the overall transfer matrix of a RPV system with a side-discharge valve can be obtained, and the magnitude of the resonant response as measured at the upstream face of the in-line valve is written as

$$\left|h_{odd}\right| = \frac{\hat{q} Z_V}{1 + \frac{Z_V}{2Z_L}\left[1 - \cos\left(\pi x_L^* \omega_r^{odd}\right)\right]} \tag{7}$$

Frequency response equations for RPV-Closed Valve systems

For *RPV-Closed Valve* systems, the pipeline sections and the leak are modeled by their transfer matrices as described in Eq. (2) and Eq. (3), respectively. The in-line valve is not included in the deviation, as it is fully closed to form the dead end. A side-discharge valve that is located at the upstream face of the closed in-line valve is used to generate the transients, and Eq. (6) is adopted to describe the input discharge perturbation produced by the side-discharge valve. Finally, the magnitude of the resonant response as measured at the upstream face of the closed in-line valve is derived as

$$\left|h_{odd}\right| = \frac{\hat{q}}{\frac{1}{2Z_L}\left[1 - \cos\left(\pi x_L^* \omega_r^{odd}\right)\right]} \tag{8}$$

RPV-Closed Valve systems can be regarded as *RPV-High Loss Valve* systems but the opening of the valve is extremely small, and accordingly the impedance of the valve is extremely high. Under this assumption, Eq. (8) can be obtained directly from Eq. (7) by rearranging the equation and setting the impedance of the valve Z_V to infinite.

Comparison between the RPV-High Loss Valve and the RPV-Closed Valve boundary conditions

Compared with the *RPV-High Loss Valve* boundary condition, the *RPV-Closed Valve* boundary condition has two limitations: firstly, the dead end boundary condition cannot always be obtained because the in-line valve in real pipelines may not seal perfectly; secondly, theoretically, the magnitude of the resonant response can be infinite for *RPV-Closed Valve* systems according to Eq. (8) (when the cosine component in the denominator equals unity). In real pipelines, the magnitude of the resonant response will not be infinite due to the effects of friction, but it will still be large. The high magnitude of resonant response can introduce risks of pipe burst and significant fluid-structure interactions. In contrast, for *RPV-High Loss Valve* systems, the maximum magnitude of resonant response is controllable and it is related to the impedance of the valve according to Eq. (7).

However, the *RPV-Closed Valve* boundary condition has its own benefits. The governing equation for the resonant response of *RPV-Closed Valve* systems [Eq. (8)] is less complex than that of systems with the *RPV-High Loss Valve* boundary condition, as the impedance of the valve Z_V is not included. As a result, theoretically less information is required for estimating the leak location and size in systems with the *RPV-Closed Valve* boundary condition.

Techniques are developed in this research for leak detection in pipelines with the *RPV-High Loss Valve* and the *RPV-Closed Valve* boundary conditions, respectively. The leak detection technique for *RPV-High Loss Valve* systems is presented first, following by the technique for *RPV-Closed Valve* systems as a special case.

Leak detection for *RPV-High Loss Valve* systems

The development of a technique for detecting leaks in *RPV-High Loss Valve* systems is presented in this section. It can be seen from Eqs (5) and (7) that the magnitude of each resonant response $|h_{odd}|$ is related to the impedance of the leak Z_L and the dimensionless location of the leak x_L^*. Provided the values of other parameters are known, including $(2\Delta H_{V0}\Delta\tau/\tau_0)$, $\hat{q}$ and Z_V, theoretically only two equations are required for solving the two unknowns, which means only two resonant responses are needed for leak location and size estimation.

In practice, however, the estimation of $(2\Delta H_{V0}\Delta\tau/\tau_0)$, $\hat{q}$ and Z_V may have errors, thus yielding errors in the estimated values of Z_L and x_L^*. This research proposes a leak location algorithm that uses solely the magnitude of the first three resonant responses, being independent of the values of $(2\Delta H_{V0}\Delta\tau/\tau_0)$, $\hat{q}$ or Z_V. However, the impedance of the leak Z_L cannot be derived using the magnitude of the first three resonant responses solely, but rather the ratio of Z_V to Z_L can be estimated.

Details about the new leak location and size estimation algorithms for *RPV-High Loss Valve* systems are described below. A sensitivity analysis is performed to confirm the robustness and applicable range of the proposed technique.

Determination of the leak location for RPV-High Loss Valve systems

In the proposed new leak location technique, all the parameters on the right hand side of Eq. (5) or Eq. (7) are assumed to be unknowns. Although there are a number of symbols on the right hand sides of these equations, it is observed that they can be categorized into three independent variables. For Eq. (5), the three variables are $\left(2\Delta H_{V0}\Delta\tau/\tau_0\right)$, Z_V/Z_L and x_L^*. For Eq. (7), they are $\hat{q}Z_V$, Z_V/Z_L and x_L^*. As a result, to solve for x_L^*, three equations are required, which means the peak values of three resonant responses are needed.

Using the inverted peak values of the first three resonant responses given by Eq. (5) or Eq. (7) (obtained with ω_r^{odd} = 1, 3 and 5 respectively), the following equation can be written:

$$\frac{\dfrac{1}{|h|_1}-\dfrac{1}{|h|_5}}{\dfrac{1}{|h|_1}-\dfrac{1}{|h|_3}}=\frac{\cos(5\pi x_L^*)-\cos(\pi x_L^*)}{\cos(3\pi x_L^*)-\cos(\pi x_L^*)} \tag{9}$$

where the subscripts '$_{odd}$' for the head responses are removed for simplicity, and the new subscripts '$_1$, $_3$ and $_5$' representing the values of ω_r^{odd} are used. Simplifying the above equation and assuming $\cos(\pi x_L^*) \neq 0 \; or \pm 1$, which means $x_L^* \neq 0$, 0.5 or 1, the following equation is obtained:

$$\frac{\left(|h|_5 - |h|_1\right)|h|_3}{\left(|h|_3 - |h|_1\right)|h|_5} = 4\cos^2(\pi x_L^*) - 1 \tag{10}$$

Eq. (10) gives the relationship between the peak values of the first three resonant responses and the location of the leak. This relationship is independent of any other parameters. In addition, x_L^* is only related to the relative sizes of the peaks, thus the absolute magnitude of the resonant response is not important. Solving Eq. (10) for x_L^* yields

$$x_L^* = \frac{1}{\pi} arc\cos\left(\pm\frac{1}{2}\sqrt{1+P_L}\right) \tag{11}$$

where P_L represents the left part of Eq. (10).

From Eq. (11), two values of x_L^* can be obtained for a specific value of P_L, provided the two values within the brackets in Eq. (11) are within the range of [-1, 1]. The summation of these two x_L^* values is unity, implying that they are two symmetric possible leak locations along the pipe. Numerical simulations performed in this research illustrate that, by comparing the size of the first two resonant responses $|h|_1$ and $|h|_3$, the alias can be eliminated. When $|h|_1 > |h|_3$, the leak is located within the range of $x_L^* \in (0, 0.5)$; while when $|h|_1 < |h|_3$, the leak is located within $x_L^* \in (0.5, 1)$. Details of the numerical simulations are given in Fig. 2 in the sensitivity analysis presented in a latter section.

Determination of the leak size for RPV-High Loss Valve systems

Once the leak location has been identified, the leak size can be determined. In the steady state, the size of the leak is related to the steady-state head H_{L0} and discharge Q_{L0} at the leak through the orifice equation

$$Q_{L0} = C_{Ld} A_L \sqrt{2gH_{L0}} \tag{12}$$

where C_{Ld} is the discharge coefficient of the leak; and A_L is the flow area of the leak orifice. To estimate the lumped leak parameter $C_{Ld}A_L$, the values of H_{L0} and Q_{L0} need to be known.

The value of H_{L0} can be estimated once the location of the leak x_L^* has been determined. The value of Q_{L0} can be calculated if the value of the leak impedance Z_L is known ($Q_{L0} = 2H_{L0} / Z_L$). However, unlike the x_L^*, the value of Z_L cannot be estimated from the magnitude of the first three resonant responses directly, but rather only the value of Z_V / Z_L can be obtained. Using Eq. (5) or Eq. (7) with ω_r^{odd} = 1 and 3, the following equation can be derived:

$$Z_L = \frac{Z_V}{2} \frac{|h|_3 \left[\cos(3\pi x_L^*) - 1\right] - |h|_1 \left[\cos(\pi x_L^*) - 1\right]}{|h|_3 - |h|_1} \tag{13}$$

where the value of Z_V can be estimated from the steady-state head loss across the valve ΔH_{V0} and the steady-state flow through the valve Q_{V0} (which in turn can be estimated from ΔH_{V0} using the orifice equation).

Compared with the process for estimating the leak location [Eq. (11)], the estimation of the leak size depends on more parameters, and the procedure is more complex. However, in practice it is more important to detect the existence of a leak and estimate its location. A sensitivity analysis is performed and presented below for the proposed leak location algorithm to confirm its robustness and applicable range.

Sensitivity analysis for the three resonant responses-based leak location algorithm

A sensitivity analysis is now performed to assess the robustness and the applicable range of the proposed three resonant responses-based leak location technique. The sensitivity analysis is based on the analysis of the total differential of x_L^*, which is presented as dx_L^*, with respect to all the dependent variables, which are the measured three resonant responses $|h|_1$, $|h|_3$ and $|h|_5$. By normalizing the total differential dx_L^* by x_L^*, the relationship between the fractional change in x_L^* (which is dx_L^*/x_L^*) and the fractional change in each dependent variable (which are $d|h|_1/|h|_1$, $d|h|_3/|h|_3$ and $d|h|_5/|h|_5$) can be obtained. The coefficient before the fractional change of a variable represents the degree of influence of this variable on the estimated x_L^*. The smaller the absolute value of the coefficient, the less sensitive the estimated x_L^* is to the corresponding dependent variable. The procedure for the total differential-based sensitivity analysis is detailed below.

Using Eq. (10), the total differential of x_L^* with respect to $|h|_1$, $|h|_3$ and $|h|_5$ can be obtained as presented in Eq. (14):

$$\frac{dx_L^*}{x_L^*} = C_1 \frac{d|h|_1}{|h|_1} + C_3 \frac{d|h|_3}{|h|_3} + C_5 \frac{d|h|_5}{|h|_5} \tag{14}$$

where the three coefficients before $d|h|_1/|h|_1$, $d|h|_3/|h|_3$ and $d|h|_5/|h|_5$ are

$$\begin{aligned} C_1 &= -\frac{2\cos(2\pi x_L^*)+1}{4\pi x_L^* \sin(2\pi x_L^*)} \frac{|h|_1\left(|h|_5 - |h|_3\right)}{\left(|h|_3 - |h|_1\right)\left(|h|_5 - |h|_1\right)} \\ C_3 &= \frac{2\cos(2\pi x_L^*)+1}{4\pi x_L^* \sin(2\pi x_L^*)} \frac{|h|_1}{\left(|h|_3 - |h|_1\right)} \\ C_5 &= -\frac{2\cos(2\pi x_L^*)+1}{4\pi x_L^* \sin(2\pi x_L^*)} \frac{|h|_1}{\left(|h|_5 - |h|_1\right)} \end{aligned} \tag{15}$$

It can be seen from Eqs (14) and (15) that, for any leak position, if the fractional changes (relative errors) in the first three peak values are the same ($d\left|h\right|_1/\left|h\right|_1 = d\left|h\right|_3/\left|h\right|_3 = d\left|h\right|_5/\left|h\right|_5$), theoretically the estimation of x_L^* is free of error ($dx_L^*/x_L^* = 0$), because the summation of the three coefficients is zero ($C_1 + C_3 + C_5 = 0$). This indicates that theoretically steady friction does not have any effects on the proposed leak location technique, because steady friction only introduces uniform reduction on the overall magnitude of the resonant response (Lee et al. 2005b).

In practice, however, due to the effects of frequency-dependent behavior, the fractional changes in the first three peak values are usually different. Therefore, it is necessary to analyze the behavior of the three coefficients in detail. When the value of x_L^* is close to 0, 0.5 or 1, the coefficients C_1, C_3 and C_5 can be much greater than unity, as shown in Eq. (15). This indicates that the estimation of x_L^* from Eq. (11) is very sensitive to variations in the peak values for these cases. As a result, when the dimensionless leak location x_L^* is close to 0, 0.5 or 1, the proposed leak location algorithm is unstable and not applicable.

For other leak positions, the values of the three coefficients in Eq. (14) vary. To study the dependence of the three coefficients on the location of the leak x_L^*, a dimensionless analysis is performed. Dividing the resonant response $\left|h_{odd}\right|$ shown in Eq. (5) [or Eq. (7)] by $\left(2\Delta H_{V0}\Delta\tau/\tau_0\right)$ (or $\hat{q}Z_V$), the resonant response can be nondimensionalized to $\left|h_{odd}\right|^*$, and the result is shown as

$$\left|h_{odd}\right|^* = \frac{1}{1 + \dfrac{Z_V}{2Z_L}\left[1 - \cos\left(\pi x_L^* \omega_r^{odd}\right)\right]} \tag{16}$$

Fig. 2 is obtained from Eq. (16), which shows how the dimensionless peak values of the first three resonant responses change when x_L^* varies from 0 to 1. The value of Z_V/Z_L is fixed to unity, which means that the impedance of the leak is the same as the impedance of the valve in the steady state. Note that the value of Z_V / Z_L can change the absolute magnitude of the FRD, but the order of the peaks remains unaffected (Lee et al. 2005a). The effects of Z_V / Z_L on the values of the three coefficients (C_1 , C_3 and C_5) is discussed later in this section.

The changing patterns of the dimensionless peak values shown in Fig. 2 are consistent with the curves shown in Fig. 8 in Lee et al. (2005a), which are dimensional rather than dimensionless. As shown in Fig. 2, the peak values are observed to intersect at five leak positions along the pipeline, dividing the pipeline into six unequal sections. Within each section, the order of the three peaks, i.e. the peak-ranking sequence, is unique. Lee et al (2005a) developed a *resonance peak-sequencing method* for locating a leak within a particular section using the rank of the measured first three resonant responses. In the current research, the rank of the first two resonant responses is used to eliminate the alias from the two possible leak locations estimated by the proposed three resonant responses-based leak location algorithm [Eq. (11)]. When $|h|_1 > |h|_3$, the leak is located within the range of $x_L^* \in (0, 0.5)$; while when $|h|_1 < |h|_3$, the leak is located within $x_L^* \in (0.5, 1)$.

The values of the coefficients C_1, C_3 and C_5 can then be estimated from Fig. 2 for various leak positions, and the results are shown in Fig. 3.

As seen in Fig. 3 and as expected, for three x_L^* ranges [0, 0.1], [0.45, 0.55] and [0.9, 1], the values of the three coefficients C_1, C_3 and C_5 are very large (values exceeding ± 10 are not displayed). This confirms the previous statement that the leak cannot be detected when it is located near x_L^* = 0, 0.5, or 1. In contrast, for leak position ranges $x_L^* \in [0.1, 0.45]$ and $x_L^* \in [0.55, 0.9]$, most values for the three coefficients are within [-1, 1]. As a result, the proposed leak location algorithm is applicable within these two ranges.

The above numerical analysis also illustrates that the proposed leak location algorithm is tolerant of measurement errors. In real applications the measurement errors in the three peak values ($d|h|_1/|h|_1$, $d|h|_3/|h|_3$ and $d|h|_5/|h|_5$) usually share the same sign. For example, unsteady friction introduces reduction to all the resonant peak values, although non-uniform. However, from Fig. 3, the values of C_1, C_3 and C_5 for any x_L^* are always a mixture of positive and negative values. According to Eq. (14), the final result of dx_L^* / x_L^* can be smaller than the summation of the measurement errors in the three peak values ($d|h|_1/|h|_1 + d|h|_3/|h|_3 + d|h|_5/|h|_5$), which indicates the fact that part of the effects of the error in the measured peak values can be cancelled out through the transfer process to the error in the estimated leak location.

From additional numerical testing, increasing Z_V / Z_L increases the robustness of the new leak location algorithm [Eq. (11)]. Although the value of Z_V / Z_L does not affect the order of the peaks, it exerts an influence on the magnitude of the resonant responses and the values of the three coefficients. When the value of Z_V / Z_L increases from 1, the difference between $|h|_1$, $|h|_3$ and $|h|_5$ increases and the values of C_1, C_3 and C_5 decrease correspondingly. In practice, the increase of Z_V / Z_L can be achieved by reducing the opening of the in-line valve. The value of Z_V will be increased accordingly, while the value of Z_L is constant when the effects of friction are ignored, and it will not change significantly even when friction is included.

In summary, the proposed three resonant responses-based leak location technique for the *RPV-High Loss Valve* system is applicable when the leak is located within $x_L^* \in [0.1, 0.45]$ or $x_L^* \in [0.55, 0.9]$. To assure the robustness of the algorithm, the opening of the in-line valve is suggested to be small to yield a large value of Z_V / Z_L.

Leak detection for *RPV-Closed Valve* systems

A leak detection technique is developed for *RPV-Closed Valve* systems, which is a special case of *RPV-High Loss Valve* systems when the opening of the valve is extremely small. The frequency response equation for an *RPV-Closed Valve* system is given in Eq. (8). Compared with Eq. (7) for an *RPV-High Loss Valve* system, the impedance of the valve Z_V is not included on the right hand side of Eq. (8). The unknowns can be regarded as $\hat{q}Z_L$ and x_L^*, so that only two equations are required to solve these two unknowns from the measured resonant responses. The requirement for the signal bandwidth is further reduced, as only the second resonant frequency needs to be covered. Details about the two resonant responses-based leak location and size estimation procedures for *RPV-Closed Valve* systems are given below.

Determination of the leak location for RPV-Closed Valve systems

As a special case of RPV systems, a single leak in a pipeline with the RPV-Closed Valve boundary condition can be detected from the magnitude of the first two resonant responses. Using Eq. (8) and substituting ω_r^{odd} with 1 and 3, the peak values of the first two resonant responses can be obtained as $|h|_1$ and $|h|_3$. Dividing $|h|_1$ by $|h|_3$, the unknown $\hat{q}Z_L$ can be eliminated, yielding an equation with a single unknown x_L^*, as shown in the equation below:

$$\frac{|h|_1}{|h|_3} = \left[2\cos(\pi x_L^*) + 1\right]^2 \qquad (17)$$

Solving the above equation for x_L^* yields

$$x_L^* = \frac{1}{\pi} arc\cos\left[\frac{1}{2}\left(\pm\sqrt{\frac{|h|_1}{|h|_3}} - 1\right)\right] \qquad (18)$$

According to Eq. (18), if $|h|_1 > |h|_3$, only one x_L^* can be obtained and it is within the range $x_L^* \in (0, 0.5)$. However, if $|h|_1 < |h|_3$, two x_L^* values may be obtained, but one of them is an alias. The two possible leak locations are both within the range $x_L^* \in (0.5, 1)$, so that the alias cannot be identified solely by using the rank of the first two resonant responses. The *resonance peak-sequencing method* would be helpful, but it requires the measurement of the third resonant response.

Notably, the three resonant responses-based leak location algorithm given in Eq. (11) for *RPV-High Loss Valve* systems is also applicable for *RPV-Closed Valve* systems, as the *RPV-Closed Valve* condition is a special case of the *RPV-High Loss Valve* condition when the impedance of the in-line valve is infinite or extremely high. One benefit of using three resonant responses is that the aliased leak location can be distinguished. On the other hand, a disadvantage is that it requires the input signal to have a wider bandwidth to cover the third resonant frequency.

Determination of the leak size for RPV-Closed Valve systems

To estimate the size of a leak, the impedance of the leak Z_L needs to be known. Once the location of the leak is estimated, the value of $\hat{q}Z_L$ can be estimated using either $|h|_1$ or $|h|_3$. Then, the value of the discharge perturbation $\hat{q}$ must be known to estimate the value of Z_L. Finally, using the value of Z_L and the orifice equation [Eq. (12)], the lumped leak parameter $C_{Ld}A_L$ can be estimated.

The value of $\hat{q}$ can be estimated from the measured pressure deviation resulting from the movement of the side-discharge valve, which is defined as the *input flow perturbation* in Lee et al. (2006). The input flow perturbation is related to the head perturbation during the generation of the transient by the Joukowsky formula. In the case where the side-discharge valve is located adjacent to a closed boundary with the valve perturbing in a pulse-like fashion, $\hat{q}$ can be estimated as $\hat{q} = -(gA/a)\Delta H$, where ΔH is the head perturbation from the mean state at the generation point.

Sensitivity analysis for the two resonant responses-based leak location algorithm

To study the robustness of the two resonant responses-based leak location algorithm, as given in Eq. (18), a sensitivity analysis is performed. The total differential dx_L^* is derived from Eq. (17) and then normalized by x_L^*, which is shown as

$$\frac{dx_L^*}{x_L^*} = C_1' \frac{d|h|_1}{|h|_1} + C_3' \frac{d|h|_3}{|h|_3} \tag{19}$$

where

$$\begin{aligned} C_1' &= -\frac{2\cos(\pi x_L^*) + 1}{4\pi x_L^* \sin(\pi x_L^*)} \\ C_3' &= \frac{2\cos(\pi x_L^*) + 1}{4\pi x_L^* \sin(\pi x_L^*)} \end{aligned} \tag{20}$$

It can be seen from Eq. (20) that the values of the two coefficients C_1' and C_3' are independent of the magnitude of the resonant responses, but rather depending only on the dimensionless leak location x_L^*. The plots for C_1' and C_3' are given in Fig. 4.

The values of C_1' and C_3' represent the sensitivity of the estimated x_L^* to the measured resonant responses $|h|_1$ and $|h|_3$ for various leak positions. Most values of C_1' and C_3' are within the range of [-1, 1] when the leak location range is within [0.2, 0.95]. Therefore, the two resonant responses-based leak location algorithm is stable and applicable when the leak is located within $x_L^* \in [0.2, 0.95]$.

Similar to the leak location algorithm using three resonant responses, the two resonant responses-based leak location algorithm is also tolerant of measurement errors, as the values of C_1' and C_3' are the same in the absolute value but always opposite in sign. According to Eq. (19), part of the effects of the frictional variations (relative errors) in $|h|_1$ and $|h|_3$ can be cancelled out if they share the same sign, which is usually the case in real applications. However, two possible leak locations may be obtained from Eq. (18) for a pair of $|h|_1$ and $|h|_3$.

The values of C_1' and C_3' for the two resonant response-based algorithm shown in Fig. 4 are small around x_L^* = 0.5, which indicates that the leak location can be estimated even if it is located at or around the middle of the pipeline. However, if the actual leak location is x_L^* = 0.5, an alias x_L^* = 1 will exist. It cannot be removed because for both x_L^* = 0.5 and 1, all the resonant responses are the same, i.e. $|h|_1 = |h|_3 = |h|_5$.

In summary, the two resonant responses-based leak location algorithm is applicable to *RPV-Closed Valve* systems when the leak is located within $x_L^* \in [0.2, 0.95]$, however, if $x_L^* \geq 0.5$, two possible leak locations can be estimated and the alias is hard to be distinguished.

Numerical verification

Numerical simulations are performed to verify the proposed three resonant responses-based leak location [Eq. (11)] and size estimation [Eq. (13)] techniques for RPV-High Loss Valve systems. The transfer matrix method is used for the numerical modeling and unsteady friction is included.

The two resonant responses-based leak location [Eq. (18)] and size estimation techniques for *RPV-Closed Valve* systems are not modeled or discussed in this section, because: the *RPV-Closed Valve* condition is just a special case of the *RPV-High Loss Valve* condition; the two resonant responses-based leak location technique has difficulty in distinguishing the aliased leak location; the leak size estimation procedure for *RPV-Closed Valve* systems is complicated; and the three resonant responses-based leak location technique is still applicable for systems with the *RPV-Closed Valve* boundary condition. However, both the three and the two resonant responses-based leak location techniques are applied to the interpretation of an experimental FRD, as presented later in the *experimental verification* section in this paper.

Unsteady friction model

Unsteady friction is included in the numerical simulations performed in this section. Compared with frictionless pipeline models or models with steady friction only, the behavior of the numerical model with unsteady friction is closer to that of real pipelines, thus yielding a better estimation of the validity of the proposed leak detection technique.

The unsteady friction model used in this research is adopted from Vítkovský et al. (2003a). Vítkovský et al. (2003a) derived the frequency-domain expression for the unsteady friction component (R_{us}) of the resistance term using the Zielke (1968) unsteady friction model and the Vardy and Brown (1996) weighting function for smooth-pipe turbulent flow, which is given below as

$$R_{us} = \frac{2j\omega}{gA}\left(\frac{1}{C} + \frac{j\omega D^2}{4\nu}\right)^{-1/2} \tag{21}$$

where ν is the kinematic viscosity and C is the shear decay coefficient, which depends on the Reynolds number of the mean flow and is given by $C = 7.41/\mathbf{Re}^{\kappa}$ and $\kappa = \log_{10}\left(14.3/\mathbf{Re}^{0.05}\right)$.

The summation of the unsteady friction component R_{us} and the steady friction component R_s composes the linearized resistance term R in Eq. (1). Together with the matrix for a leak Eq. (3) and the matrix for an oscillating valve Eq. (4), the governing equation for the resonant response at the upstream face of the valve can be derived. The numerical studies described in the following subsections are based on this numerical pipeline model.

Pipeline models with steady friction only are not considered in the numerical study. Steady friction is not dependent on frequency and only yields a uniform reduction on the overall magnitude of the frequency response. According to the sensitivity analysis shown in Eq. (14), the uniform distortion due to steady friction does not have any effects on the accuracy of the estimated leak location.

Case study

A case study is performed on a pipeline with a leak located at $x_L^* = 0.2$, where the unsteady friction model described in the previous subsection is used. The system layout is given in Fig. 1. The in-line valve is used to generate the transient, and it is assumed to have a small opening in the steady state and connected to the atmosphere at the downstream side. The parameters used for the numerical simulations are listed in Table 1 below.

The frequency response diagrams (FRDs) for the case study ($x_L^* = 0.2$) are obtained numerically using the transfer matrix method. The results are presented in Fig. 5, where the FRD in the solid line is for the pipeline with the system parameters shown in Table 1 and with unsteady friction (Vítkovský et al. 2003a); the FRD in the dotted line is for the same pipeline but under a frictionless assumption. The FRDs in Fig. 5 are nondimensionalized, where the y-axis represents the dimensionless head response that is nondimensionalized by dividing the dimensional resonant response by the active input $\left(2\Delta H_{V0}\Delta\tau / \tau_0\right)$, and the x-axis denotes the relative angular frequency $\omega_r = \omega / \omega_{th}$.

From Fig. 5, the dimensionless peak values for the first three resonant responses are $|h|_1$ = 0.912, $|h|_3$ = 0.601 and $|h|_5$ = 0.496 for the frictionless simulation (the dotted line), and $|h|_1^{us}$ = 0.821, $|h|_3^{us}$ = 0.542 and $|h|_5^{us}$ = 0.446 for the simulation with unsteady friction (the solid line). Using Eq. (11) and $|h|_1^{us}$, $|h|_3^{us}$ and $|h|_5^{us}$, the possible dimensionless leak locations are estimated as $\left(x_L^*\right)^{us}$ = 0.199 or $\left(x_L^*\right)^{us}$ = 0.801. Then using the rank of the first two resonant response $\left|h\right|_1^{us} > \left|h\right|_3^{us}$, it is concluded that the leak should be within the range of (0, 0.5). Therefore, the leak is confirmed to be located at $\left(x_L^*\right)^{us}$ = 0.199.

Compared with the actual leak location x_L^* = 0.2 m, $\left(x_L^*\right)^{us}$ is accurate as it only has a relative deviation of $\left[\left(x_L^*\right)^{us} - x_L^*\right]/x_L^* \times 100\,\%$ = -0.5 %. This deviation is much smaller than the deviation between the numerical peak values for the unsteady friction model ($\left|h\right|_1^{us}$, $\left|h\right|_3^{us}$ and $\left|h\right|_5^{us}$) and the results for the frictionless model ($\left|h\right|_1$, $\left|h\right|_3$ and $\left|h\right|_5$). In addition, the value of dx_L^*/x_L^* is calculated as -0.2 % using the estimated $\left(x_L^*\right)^{us}$, which is consistent with the result of Eq. (14) when the numerical peak values are substituted.

The impedance of the in-line valve is calculated as $Z_V = 1.78\times10^4$ s/m^2 from the steady-state analysis of the pipeline system shown in Table 1. The impedance of the leak is then estimated from Eq. (13) using the numerical results for the simulation with unsteady friction [$\left(x_L^*\right)^{us}$, $\left|h\right|_1^{us}$, $\left|h\right|_3^{us}$ and $\left|h\right|_5^{us}$] and it is Z_L = 1.75×10^4 s/m^2. Using Z_L and assuming that the steady-state head at the leak H_L is the same as the reservoir head H_r, finally the lumped leak parameter can be estimated from Eq. (12) and it is $\left(C_{Ld}A_L\right)^{us}$ = 1.42×10^{-4} m^2. Compared with the theoretical leak size given in Table 1, the estimation is accurate.

The above numerical case study with x_L^* = 0.2 and incorporating unsteady friction shows that the leak location and size are estimated accurately using the proposed three resonant responses-based leak detection technique. To study the behavior of the proposed leak detection technique for other leak positions, additional numerical testing is performed and reported in the following subsection.

Simulations for various leak locations

Numerical simulations are performed on pipelines with the dimensionless leak location x_L^* varying from 0.01 to 0.99, with a step of 0.01 each. The system parameters used in these simulations are the same as those given in Table 1. Unsteady friction is included in all the numerical simulations.

The relative deviation between the estimated leak location and the corresponding actual leak location is estimated for each simulation. Meanwhile, for each of the estimated leak size, the relative deviation from the actual leak size is also estimated. The relative deviation for the estimated leak size is defined as $\left[\left(C_{Ld}A_L\right)^{us} - C_{Ld}A_L\right] \Big/ C_{Ld}A_L \times 100\,\%$. The curves of the relative deviation for the estimated leak location and the estimated leak size are given in Fig. 6.

The curves presented in Fig 6 are not continuous. One reason for the discontinuity is that the data out of the bounds of the *y*-axis are not shown, and another reason is that the leak location algorithm Eq. (11) and/or the leak impedance estimation algorithm Eq. (13) are not applicable mathematically when the leak is located at some specific positions. It can be seen from Fig. 6 that when the leak is actually located within $x_L^* \in [0.15, 0.4]$ or $x_L^* \in [0.6, 0.9]$, the accuracy of the estimated leak location $\left(x_L^*\right)^{us}$ is acceptable (within ± 5%). In contrast, the estimated leak size is less accurate, as expected, and underestimated most times.

The numerical simulations indicate that the proposed three resonant responses leak location algorithm is applicable for pipelines with unsteady friction. The relative deviations of the estimated leak locations (solid lines in Fig. 6) are consistent with the results of Eq. (14) in the sensitivity analysis. However, compared with the theoretical applicable ranges $x_L^* \in [0.1, 0.45]$ and $x_L^* \in [0.55, 0.9]$ for frictionless pipes given in the sensitivity analysis, when the effects of unsteady friction are considered, the applicable ranges is slightly reduced to $x_L^* \in [0.15, 0.4]$ and $x_L^* \in [0.6, 0.9]$. The estimation of the leak size is less accurate, and it is usually underestimated compared with the actual leak size. The proposed leak detection technique is further verified using an experimentally determined FRD in the following section.

Experimental verification

The proposed three and two resonant responses-based leak location techniques are verified using an experimentally determined FRD. The laboratory experiments were conducted by Lee et al. (2006) in the Robin Hydraulics Laboratory at the University of Adelaide. The methods for extracting the FRD of a real pipeline have been discussed in detail in Lee et al. (2006). The system configuration and experimental data presented in Lee et al. (2006) are also described briefly in the subsection below.

System configuration and experimental data

The experimental pipeline was a copper pipeline in a tank-pipeline-(in-line) valve configuration. The length of the pipe is L = 37.53 m and the internal diameter is D = 0.022 m. The in-line valve is fully closed, so the pipeline system had a *RPV-Closed Valve* boundary condition. The upstream water tank is pressurized by air and the steady-state pressure head is H_r = 38.09 m. The wave speed in the experimental pipeline was a = 1328 m/s determined by experiment. A side-discharge valve was located at the upstream face of the closed in-line valve to generate the transient excitation (a pulse signal). A free discharging orifice with a diameter of 1.5 mm ($C_{Ld}A_L = 1.6\times10^{-6}\,\mathrm{m}^2$) was located at 28.14 m downstream from the reservoir to simulate the leak, thus the actual dimensionless leak location was x_L^* = 0.75.

The experimentally determined FRD was presented as Fig. 17 in Lee et al. (2006). The peak values for the first resonant responses are estimated as $|h|_1^{lab} = 3.05\times10^6$ m^{-2}s,

$|h|_3^{lab} = 7.75 \times 10^6$ m^{-2}s and $|h|_5^{lab} = 5.35 \times 10^6$ m^{-2}s from the experimental FRD. They represent the head response per unit discharge input [i.e. $\hat{q}$ = 1 m^3/s in Eq. (8)].

Leak location using the three resonant responses-based technique

Using the three resonant responses-based leak location technique given in Eq. (11), the dimensionless leak location is estimated as $\left(x_L^*\right)^{lab}$ = 0.27 or 0.73. The rank of the peak values of the first two resonant responses is $|h|_1^{lab} < |h|_3^{lab}$, so that the leak should be within a dimensionless range of $(0.5, 1)$. As a result, $\left(x_L^*\right)^{lab}$ = 0.73 is adopted. Compared with the actual dimensionless leak location x_L^*, the absolute error in the estimated x_L^* is $\left(x_L^*\right)^{lab} - x_L^*$ = - 0.02, and the relative error is $\left[\left(x_L^*\right)^{lab} - x_L^*\right] \big/ x_L^* \times 100\,\%$ = -2.7 %. The size of the leak is not estimated, because the proposed leak size estimation formula [Eq. (13)] is not applicable to the experimental pipeline with the *RPV-Closed Valve* boundary condition.

Leak location and size estimation using the two resonant responses-based technique

For the two resonant responses-based leak location technique, Eq. (18) is used. The dimensionless location of the leak is estimated as $\left(x_L^*\right)^{lab}$ = 0.56 or 0.80. The alias cannot be removed. For the estimation $\left(x_L^*\right)^{lab}$ = 0.80 which is closer to the actual location, it is less accurate than the estimation derived from the three responses-based leak location technique.

To determine the size of the leak, the impedance of the leak is determined first. It is estimated as $Z_L = 2.53 \times 10^6$ s/m^2 by substituting the first resonant response $|h|_1^{lab} = 3.05 \times 10^6$ m^{-2}s and the unit discharge perturbation $\hat{q}$ = 1 m^3/s into Eq. (8). Then, under the assumption that the steady-state head at the leak is the same as the steady-state head at the reservoir ($H_{L0} = H_r = 38.09$ m), the steady-state flow at the leak is estimated as $Q_{L0} = 3.01 \times 10^{-5}$ m^3/s. Finally, the lumped leak size is estimated as $\left(C_{Ld} A_L\right)^{lab} = 1.1 \times 10^{-6}$ m^2 using the orifice equation Eq. (12). Compared with the theoretical leak size ($C_{Ld} A_L = 1.6 \times 10^{-6}$ m^2), the estimated size is significantly smaller.

Summary of experimental verification

The experimental verification illustrates that the proposed leak detection technique is applicable to pipelines in controlled laboratory conditions. The location of the leak is estimated successfully using either the three or the two resonant responses-based algorithm. The leak location estimated from the three resonant responses-based algorithm is accurate, with an absolute error of 2 % of the total pipe length. However, the two resonant responses-based algorithm yields less accuracy. The size of the leak is estimated from the two resonant responses-based algorithm, but the estimated leak size is smaller than the theoretical value.

The error in the estimates comes from the distortion in the experimentally determined FRD, which in turn may be mainly sourced from the effects of frequency-dependent behavior in the experimental pipeline, such as unsteady friction. For pipelines with longer length in the field, the fundamental frequency is usually significantly lower and the effects of unsteady friction on the first three resonant responses will be relatively small. As a result, it is expected that the proposed leak location technique is also applicable in field applications.

Challenges in field applications

The proposed leak detection technique has been verified by numerical studies and controlled laboratory experiments; however, some challenges may exist for application of the proposed methodology in the field. The proposed technique is designed for the detection of a single leak in a single pipeline, while in the field, complex pipeline networks and multiple leaks may exist.

Lee et al. (2005a) have studied how to extract the FRD for a branched pipe network. By closing the valve at one end of the pipe section, an individual pipeline can be partially separated from the network. A side-discharge valve located adjacent to the closed valve is then used to generate a transient pulse, and a pressure transducer located at the same location as the generator is used to measure the transient pressure trace. By assuming that a reservoir exists at the open boundary, and using signal processing, the FRD of the specified pipe section can be obtained (Lee et al. 2005a).

When multiple leaks exist in a single pipeline, three resonant responses are not sufficient to be able to determine the location of all the leaks. In this case, more resonant responses need to be measured and further investigation is required. Nevertheless, using the first three resonant responses, the method proposed in this paper can determine whether the pipe is leaking or not.

Another challenge in the application of the newly proposed method is that the shape of the leak may have some impact on the accuracy of the detection. In the numerical study and the experimental verification presented in this paper, a leak is simulated by an orifice with a circular opening. If the leak has a different shape, Eq. (12) as used in this paper cannot accurately describe the relationship between the head and the flow through the leak. As a result, the estimation of the size of the leak will be in error. However, theoretically the relative size of the first three resonant responses will not be affected, so that the location of the leak can still be determined accurately. More experiments are necessary to study the effects of the shape of a leak.

Conclusions

A novel frequency response diagram (FRD)-based leak location and size estimation technique is proposed in this research. It is suitable for detecting of a single leak in single pipelines with a reservoir-pipeline-valve (RPV) configuration. Instead of using the sinusoidal leak-induced patterns on the FRD as in traditional techniques, the new technique only uses the magnitude of the first three resonant responses.

A RPV-high loss valve configuration is suggested for the extraction of the FRD. A side-discharge valve is used to generate an impulse transient excitation, which is located at the upstream face of a high loss in-line valve at the end of the pipe. A pressure transducer is located at the same location as the side-discharge valve to measure the transient pressure. The opening of the in-line valve should be small enough to make the leak-induced distortion obvious in the first three harmonics. In practice, this can be achieved by trial-and-error. In addition to the measured transient pressure, the steady-steady head and flow at the in-line valve, the head at the reservoir, the length and internal diameter of the pipe, and the wave speed in the pipe need to be known.

The requirement for the bandwidth of the transient excitation is reduced to five times of the fundamental frequency of the pipeline under test, because only the first three resonant responses are used. In addition, the distortion in the measured FRD due to unsteady friction does not need to be corrected before applying the leak detection algorithm, because the effects of unsteady friction is not significant for the first three resonant responses, and part of the effects are cancelled out through the calculation for leak location. Moreover, only the relative sizes of the first three resonant responses are required, rather than the absolute values of the frequency response. This is a great advantage, as it can simplify the procedure for determining the FRD and avoids error introduced through intermediate calculations. For example, the voltage output from a pressure transducer can be used in the calculation directly, avoiding the transfer from voltage data to pressure data.

When the in-line valve at the end of the pipeline is fully closed, the requirement for the number of resonant responses can be reduced to two. However, two possible leak locations may be obtained from a specific FRD, and the alias is hard to remove.

Numerical simulations with unsteady friction performed in this research show that the three resonant responses-based leak location technique is applicable when the actual leak is located within the dimensionless range of $x_L^* \in [0.15, 0.4]$ or $[0.6, 0.9]$. Within the applicable ranges, the relative deviation between the estimated leak location and the actual location is within ± 5 %. However, the estimated size of the leak is less accurate, and shown to be underestimated most times.

The proposed leak detection technique is also verified using an experimentally determined FRD. The experimental verification indicates that the proposed technique is applicable to real pipelines in controlled laboratory condition, even though the pipeline is short and the effects of unsteady friction is relatively high. The three resonant responses-based technique performs better than the two resonant responses-based technique. For pipelines with longer length in the field, the fundamental frequency of the pipeline is much lower and the effects of unsteady friction on the first three resonant responses will be relatively small. It is expected that the proposed three resonant responses-based technique leak detection technique is also applicable in field applications, provided the first three resonant responses can be measured successfully.

Acknowledgements

The research presented in this paper has been supported by the Australia Research Council through the Discovery Project Grant DP1095270. The first author thanks the Chinese Scholarship Council and the University of Adelaide for providing a joint postgraduate scholarship.

Notations

The following symbols are used in this paper:

A = inside pipe cross sectional area;

a = wave speed;

A_L = area of a leak orifice;

C = shear decay coefficient;

C_1, C_3, C_5 = coefficients used in Eqs (14);

C_1', C_3' = coefficients used in Eqs (19);

C_{Ld} = coefficient of discharge for a leak orifice;

D = internal pipe diameter;

f = Darcy-Weisbach friction factor;

g = gravitational acceleration;

H_0 = steady-state head;

H_r = reservoir head;

H_{L0} = steady-state head at a leak orifice;

h = complex head amplitude;

$|h_{odd}|$ = amplitude of head fluctuation at the odd harmonics;

$|h|_1$, $|h|_3$, $|h|_5$ = amplitude of the head oscillation at the first, the third and the fifth harmonics;

j = imaginary unit, $\sqrt{-1}$;

L = total length of pipe;

L_1, L_2 = lengths of the two pipe sections divided by a leak;

P_L = left part of Eq. (10);

Q_0 = steady-state discharge;

Q_{L0} = steady-state flow out of a leak;

Q_{V0} = steady-state flow through a valve;

q = complex discharge amplitude;

$\hat{q}$ = discharge perturbation;

R = linearised resistance term;

$\mathbf{R_e}$ = Reynolds number;

R_s, R_{us} resistance factor components for steady friction and unsteady friction;

x_L^* = dimensionless position of a leak;

Z_C = characteristic impedance of a frictionless pipe;

Z_L = hydraulic impedance of a leak orifice;

Z_P = the characteristic impedance of a pipe;

Z_V = hydraulic impedance of a steady-state valve;

Superscripts:

* = dimensionless values;

^{lab} sourced from laboratory experiments;

^{n}, $^{n+1}$ the upstream and the downstream position of a pipe;

$_{us}$ effects of unsteady friction are included;

Greek symbols:

ΔH = head perturbation from the mean state at the generation point;

ΔH_{V0} = steady-state head loss across a valve;

$\Delta \tau$ = amplitude of the dimensionless valve-opening oscillation;

κ = coefficient in Eq. (21);

μ = propagation operator;

ν = kinematic viscosity;

τ_0 = mean dimensionless valve-opening coefficient, centre of oscillation;

ω, ω_r = angular frequency and dimensionless relative angular frequency;

ω^{odd}, ω_r^{odd} = angular frequency and relative angular frequency for odd harmonics;

ω_{th} = fundamental angular frequency for a reservoir-pipeline-valve system;

Reference

Beuken, R. H. S., Lavooij, C. S. W., Bosch, A., and Schaap, P. G. (2006). "Low leakage in the Netherlands confirmed." *Proceedings of the Water Distribution Systems Analysis Symposium 2006*, ASCE, Reston, VA.

Brunone, B. (1999). "Transient test-based technique for leak detection in outfall pipes." *Journal of Water Resources Planning and Management*, 125(5), 302-306.

Chaudhry, M. H. (1987). *Applied Hydraulic Transients*, Van Nostrand Reinhold Company Inc, New York.

Collins, R. P., Boxall, J. B., Karney, B. W., Brunone, B., and Meniconi, S. (2012). "How severe can transients be after a sudden depressurization?" *Journal - American Water Works Association*, 104(4), E243-E251.

Colombo, A. F., and Karney, B. W. (2002). "Energy and costs of leaky pipes toward comprehensive picture." *Journal of Water Resources Planning and Management*, 128(6), 441-450.

Colombo, A. F., Lee, P., and Karney, B. W. (2009). "A selective literature review of transient-based leak detection methods." *Journal of Hydro-environment Research*, 2(4), 212-227.

Covas, D., Ramos, H., and Betamio de Almeida, A. (2005). "Standing wave difference method for leak detection in pipeline systems." *Journal of Hydraulic Engineering*, 131(12), 1106-1116.

Duan, H.-F., Lee, P. J., Ghidaoui, M. S., and Tung, Y.-K. (2011). "Leak detection in complex series pipelines by using the system frequency response method." *Journal of Hydraulic Research*, 49(2), 213-221.

Eiswirth, M., and Burn, L. S. (2001). "New methods for defect diagnosis of water pipelines." *Proceedings of the 4th International Conference on Water Pipeline Systems*, BHR Group, Cranfield, Bedfordshire, UK, 137-150.

Ferrante, M., and Brunone, B. (2003a). "Pipe system diagnosis and leak detection by unsteady-state tests. 2. wavelet analysis." *Advances in Water Resources*, 26(1), 107-116.

Ferrante, M., and Brunone, B. (2003b). "Pipe system diagnosis and leak detection by unsteady-state tests. 1. harmonic analysis." *Advances in Water Resources*, 26(1), 95-105.

Fuchs, H. V., and Riehle, R. (1991). "Ten years of experience with leak detection by acoustic signal analysis." *Applied Acoustics*, 33(1), 1-19.

Goh, J. H., Shaw, A., Cullen, J. D., Al-Shamma'A, A. I., Oliver, M., Vines, M., and Brockhurst, M. (2011). "Water pipe leak detection using electromagnetic wave sensor for the water industry." *Proceedings of the 2011 IEEE Symposium on Computers and Informatics*, IEEE Computer Society, Washington, DC, 290-295.

Inaudi, D., Belli, R., and Walder, R. (2008). "Detection and localization of micro-leakages using distributed fiber optic sensing." *Proceedings of the 2008 7th International Pipeline Conference*, ASME, New York, NY, 599–605.

Jönsson, L., and Larson, M. (1992). "Leak detection through hydraulic transient analysis." In *Pipeline Systems*, B. Coulbeck and E. P. Evans, eds., Kluwer Academic Publishers, 273-286.

Karim, M. R., Abbaszadegan, M., and Lechevallier, M. (2003). "Potential for pathogen intrusion during pressure transients." *Journal of American Water Works Association*, 95(5), 134-146.

Lambert, A. O. (2002). "International report: Water losses management and techniques." *Water Science and Technology: Water Supply*, 2(4), 1-20.

Lee, P. J., Vítkovský, J. P., Lambert, M. F., Simpson, A. R., and Liggett, J. A. (2005a). "Frequency domain analysis for detecting pipeline leaks." *Journal of Hydraulic Engineering*, 131(7), 596-604.

Lee, P. J., Vítkovský, J. P., Lambert, M. F., Simpson, A. R., and Liggett, J. A. (2005b). "Leak location using the pattern of the frequency response diagram in pipelines: a numerical study." *Journal of Sound and Vibration*, 284(3-5), 1051–1073.

Lee, P. J., Lambert, M. F., Simpson, A. R., Vítkovský, J. P., and Liggett, J. A. (2006). "Experimental verification of the frequency response method for pipeline leak detection." *Journal of Hydraulic Research*, 44(5), 693–707.

Lee, P. J., Vítkovský, J. P., Lambert, M. F., Simpson, A. R., and Liggett, J. A. (2007). "Leak location in pipelines using the impulse response function." *Journal of Hydraulic Research*, 45(5), 643-652.

McIntosh, A. C., and Yniguez, C. E. (1997). *Second Water Utilities Data Book : Asian and Pacific Region*, Asian Development Bank, Manila, Philippines.

Meniconi, S., Brunone, B., Ferrante, M., Berni, A., and Massari, C. (2011). "Experimental evidence of backflow phenomenon in a pressurised pipe." *Proceedings of the Computing and Control for the Water Industry 2011*, University of Exeter, Exeter, UK.

Mpesha, W., Gassman, S. L., and Chaudhry, M. H. (2001). "Leak detection in pipes by frequency response method." *Journal of Hydraulic Engineering*, 127(2), 134-147.

Mutikanga, H. E., Sharma, S., and Vairavamoorthy, K. (2009). "Water loss management in developing countries: Challenges and prospects." *Journal of American Water Works Association*, 101(12), 57-68.

Nixon, W., and Ghidaoui, M. S. (2006). "Range of validity of the transient damping leakage detection method." *Journal of Hydraulic Engineering*, 132(9), 944-957.

Puust, R., Kapelan, Z., Savic, D. A., and Koppel, T. (2010). "A review of methods for leakage management in pipe networks." *Urban Water Journal*, 7(1), 25 - 45.

Sattar, A. M., and Chaudhry, M. H. (2008). "Leak detection in pipelines by frequency response method." *Journal of Hydraulic Research, IAHR*, 46(sup 1), 138-151.

Tafuri, A. N. (2000). "Locating leaks with acoustic technology." *Journal of American Water Works Association*, 92(7), 57-66.

Vardy, A. E., and Brown, J. M. (1996). "On turbulent, unsteady, smooth pipe friction." *7th International Conference on Pressure Surges and Fluid Transients in Pipelines and Open Channels*, Mechanical Engineering Publications, London, UK, 289-311.

Vítkovský, J. P., Bergant, A., Simpson, A. R., and Lambert, M. F. (2003a). "Frequency-domain transient pipe flow solution including unsteady friction." *Pumps, Electromechanical Devices and Systems Applied to Urban Water Management: Proceedings of the International Conference*, A. A. Balkema Publishers, Lisse, The Netherlands, 773-780.

Vítkovský, J. P., Lee, P. J., Spethens, M. L., Lambert, M. F., Simpson, A. R., and Liggett, J. A. (2003b). "Leak and blockage detection in pipelines via an impulse response method." *Pumps, Electromechanical Devices and Systems Applied to Urban Water Management: Proceedings of the International Conference*, A. A. Balkema Publishers, Lisse, The Netherlands, 423–430.

Wylie, E. B., and Streeter, V. L. (1993). *Fluid Transients in Systems*, Prentice Hall Inc., Englewood Cliffs, New Jersey, USA.

Zielke, W. (1968). "Frequency-dependent friction in transient pipe flow." *Journal of Basic Engineering, ASME*, 90(1), 109-115.

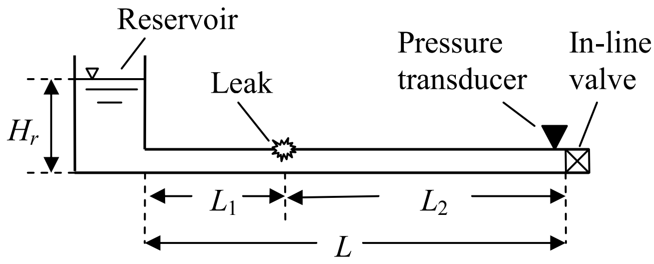

Fig. 1. A reservoir-pipeline-valve system with a leak.

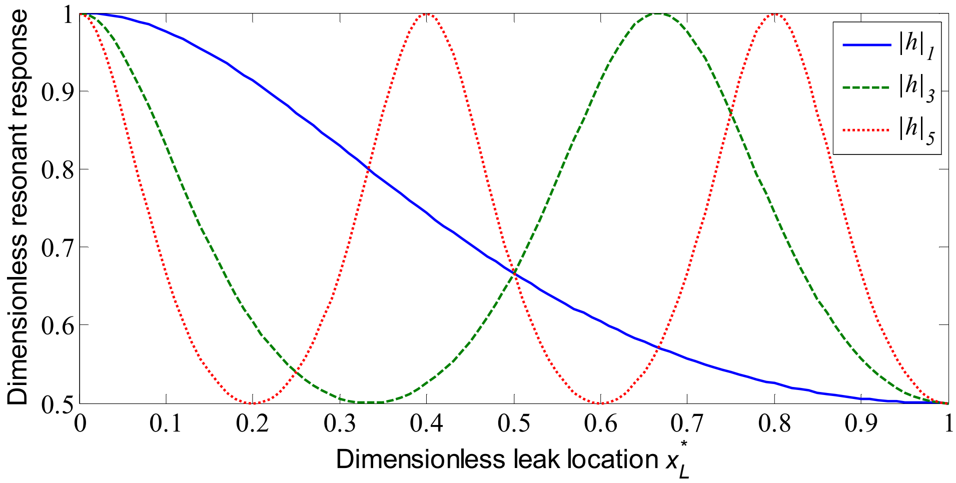

Fig. 2 Impact of the dimensionless leak location x_L^* on the dimensionless peak values of the first three resonant responses, with $Z_V / Z_L = 1$.

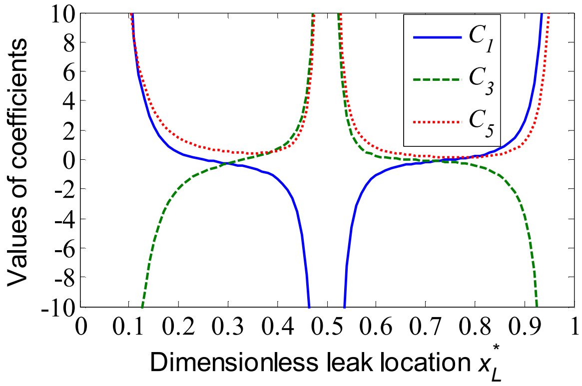

Fig. 3 Impact of the dimensionless leak location x_L^* on the three coefficients C_1, C_3 and C_5 in Eq. (14), with $Z_V / Z_L = 1$.

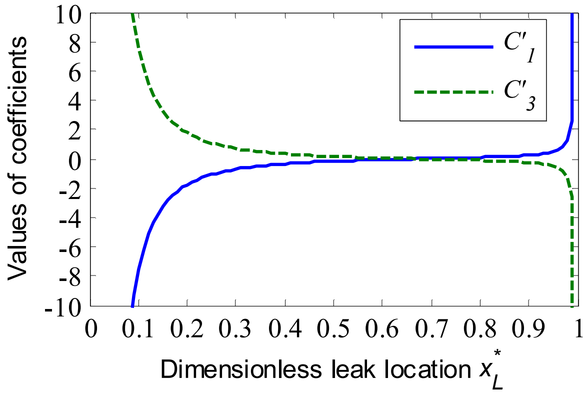

Fig. 4 Impact of the dimensionless leak location x_L^* on the two coefficients C_1 and C_3 in Eq. (19).

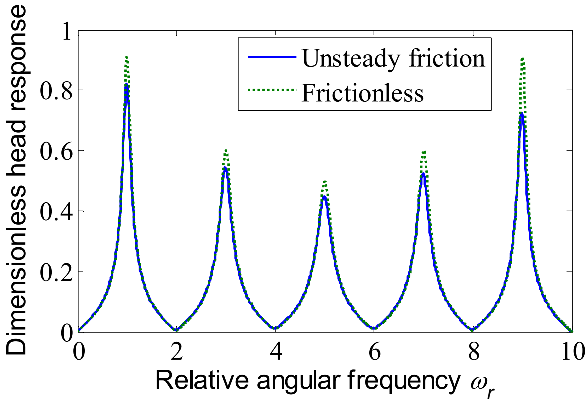

Fig. 5 Numerical FRDs for the case study $x_L^* = 0.2$.

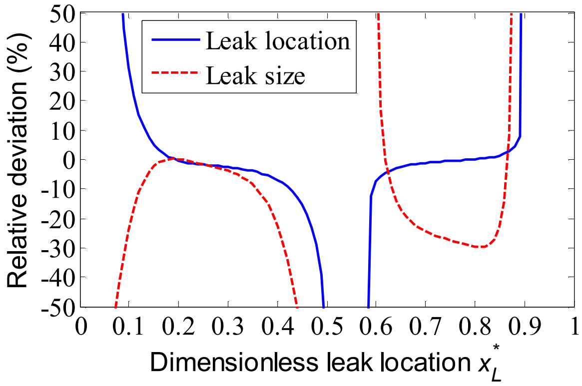

Fig. 6 The relative deviation between the estimated leak location and the actual leak location (solid lines), and the relative deviation between the estimated leak size and the actual leak size (dashed lines).

Table 1. System parameters for the numerical simulations

Parameter	Value
H_r	30 m
Q_{V0}	0.0034 m^3/s
L	2000 m
D	0.3 m
a	1200 m/s
f	0.02
$\Delta\tau / \tau_0$	0.05
$C_{Ld} A_L$	1.41×10^{-4} m^2